Deep-Sea Research II 81-84 (2012) 3–17

Contents lists available at ScienceDirect

Deep-Sea Research II

journal homepage: www.elsevier.com/locate/dsr2

Latitudinal variation of phytoplankton communities in the western Arctic Ocean

Hyoung Min Joo [a,d], Sang H. Lee [b,*], Seung Won Jung [c], Hans-Uwe Dahms [d], Jin Hwan Lee [d,*]

[a] Korea Polar Research Institute, KORDI, Songdo Techno Park, Incheon 406-840, South Korea
[b] Department of Oceanography, Pusan National University, 30, Jangjeon-dong, Busan 609-735, South Korea
[c] Korea Ocean Research & Development Institute, Geoje 656-830, South Korea
[d] Green Life Science Department, College of Natural Science, Sangmyung University, 7 Hongij-dong, Jongno-gu, Seoul 110-743, South Korea

ARTICLE INFO

Available online 6 June 2011

Keywords:
Phytoplankton
Arctic
Biodiversity
Abundance
Biovolume
Canadian Basin
Bering and Chukchi Seas

ABSTRACT

Recent studies have shown that photosynthetic eukaryotes are an active and often dominant component of Arctic phytoplankton assemblages. In order to explore this notion at a large scale, samples were collected to investigate the community structure and biovolume of phytoplankton along a transect in the western Arctic Ocean. The transect included 37 stations at the surface and subsurface chlorophyll *a* maximum (SCM) depths in the Bering Sea, Chukchi Sea, and Canadian Basin from July 19 to September 5, 2008. Phytoplankton (>2 μm) were identified and counted. A cluster analysis of abundance and biovolume data revealed different assemblages over the shelf, slope, and basin regions. Phytoplankton communities were composed of 71 taxa representing Dinophyceae, Cryptophyceae, Bacillariophyceae, Chrysophyceae, Dictyochophyceae, Prasinophyceae, and Prymnesiophyceae. The most abundant species were of pico- to nano-size at the surface and SCM depths at most stations. Nano- and pico-sized phytoplankton appeared to be dominant in the Bering Sea, whereas diatoms and nano-sized plankton provided the majority of taxon diversity in the Bering Strait and in the Chukchi Sea. From the western Bering Sea to the Bering Strait, the abundance, biovolume, and species diversity of phytoplankton provided a marked latitudinal gradient towards the central Arctic. Although pico- and nano-sized phytoplankton contributed most to cell abundance, their chlorophyll *a* contents and biovolumes were less than those of the larger micro-sized taxa. Micro-sized phytoplankton contributed most to the biovolume in the largely ice-free waters of the western Arctic Ocean during summer 2008.

1. Introduction

Phytoplankton data in the western high Arctic are limited. This holds particularly true for seasonal changes in composition and quantitative measurements of the microalgal communities, owing to limited access to this part of the world's oceans (Shirshov, 1982; Ingram et al., 2002). Hill et al. (2005) studied microalgal composition at higher taxonomic levels with size-fractionated HPLC analysis of pigments (see Zapata et al., 2000), whereas quantitative data were limited to measurements of chlorophyll *a* concentrations.

Phytoplankton communities and their contribution to primary production in this area of the Arctic are controlled by seasonal environmental changes in solar irradiation, ice cover, water temperature, and vertical stratification, as well as by the inflow of warm Pacific waters through the Bering Strait (Weingartner et al., 2005; Wang et al., 2006). Waters from the south influence the timing of the seasonal ice melting in spring as well as ice formation in the fall, which is different from other Arctic shelves. These warm and nutrient-rich waters flow northwards with the Anadyr Current through the Bering Sea into the Chukchi Sea (Springer et al., 1996; Shiomoto et al., 2002; Carmack and Wassmann, 2006). This northward flow is caused by a sea-level difference between the Bering Sea and the Arctic Ocean (Roach et al., 1995). There are two current regimes north of the Bering Strait. Along the northeastern coast of Alaska, the Alaska coastal current (ACC) flows as a low-salinity, nutrient-poor current branch. To the west there is a nutrient-rich, high-salinity branch flowing northwards (Wang et al., 2005). As a result, primary production rates are among the highest in the southwestern Chukchi Sea (Springer and McRoy, 1993), while there is only modest primary production on the outer Chukchi Shelf that drops towards the Canadian Basin (Chen et al., 2003; Wang et al., 2005). The Pacific inflow through the Bering Strait varies seasonally due to climatic factors; the resulting dynamic current structure influences the ecosystems of the Chukchi Shelf and western shelf

* Corresponding authors.
E-mail address: sanglee@pusan.ac.kr (S.H. Lee).

0967-0645/$ - see front matter © 2011 Elsevier Ltd. All rights reserved.
doi:10.1016/j.dsr2.2011.06.004

regions of the Beaufort Sea (Macklin et al., 2002). The variability of the pelagic environment affects phytoplankton and controls their taxonomic composition, abundance, biomass, *in situ* primary production, and successional dynamics (Lee et al., 2007; Ardyna et al., 2008).

As ice retreats in the western Arctic, the phytoplankton community develops seasonally and phytoplankton abundance increases (Comiso, 2002). Since sea ice retreats via indentations in the melting sea ice, it contributes to the patchiness of the phytoplankton distribution. Particularly along the ice edge, blooms are common due to wind-driven upwelling (Wang et al., 2005). River discharge additionally contributes to the nutrient supply (Shiklomanov et al., 2002). On the other hand, though, rivers might also decrease available light by adding suspended sediment and colored dissolved organic matter from river runoff.

The combination of seasonally variable environmental factors and current flow through the Bering Strait results in temporal and spatial variability of water mass characteristics in this region (Olson and Strom, 2002; Weingartner et al., 2005). Whereas pelagic phytoplankton provide most of the primary production over the shelf and slope in the Chukchi Sea, ice algae are only important here during a short period at the beginning of the spring transition (Hill and Cota, 2005). Since the Bering and Chukchi Seas represent the entrance of Pacific waters into the entire Arctic Basin, it is essential to know the extent of microalgal variability and the factors that affect it on the shelf and slope of the Arctic Ocean (Codipoti et al., 2005; Grebmeier et al., 2006a, b; Sukhanova et al., 2006).

Previous taxonomic analysis of samples in the western Arctic Ocean indicated that populations on the Chukchi Shelf are often dominated by centric diatoms in summer (Booth et al., 2002). Spatial and temporal variations in phytoplankton community structure are commonly caused by differences in water-column irradiance and nutrient concentrations. Another factor emphasized by Hill et al. (2005) is high nutrient availability in surface waters of the western Arctic Ocean in spring. Coverage by annual sea ice causes light limitation of algal growth (Hill et al., 2005). The study of Tremblay and Gagnon (2009) suggests that changes in the vertical nutrient distribution of the water column would affect the larger phytoplankton fraction more than the smaller fraction. However, interannual environmental variability can be considerable in the western Arctic and needs to be considered in the context of rapidly declining Arctic perennial ice cover during the last two decades (Wassmann et al., 2006). According to Wang et al. (2005), phytoplankton biomass increased much earlier in the Beaufort Sea when sea ice decreased early in the year. These authors demonstrated that yearly chlorophyll fluctuations showed biomass peaks up to 2 months later in cold years accompanied by more extensive ice cover.

The aim of the present study was to characterize the systematic composition of phytoplankton assemblages, their distribution, abundance, biovolume, and size composition and associate them with varying abiotic factors during a limited period of time in summer 2008 in the western Arctic Ocean. The main objective was to find large-scale latitudinal changes in phytoplankton communities at the surface and subsurface chlorophyll *a* maximum depths from the southwestern Bering Sea to the central Canadian Basin.

2. Materials and methods

2.1. Study sites and sampling

The data were collected in the western Arctic from 19 July to 5 September 2008; this period is hereafter referred to as late summer. The study region encompassed the area between 53°N and 85°N, and 169°E and 143°W (Fig. 1). Phytoplankton samples were collected as part of CHINARE 2008 aboard the Chinese icebreaker R/V *Xuelong* in three regions: the Bering Sea, the Chukchi Sea, and the Canadian Basin. A total of 37 stations were visited, comprising 17 stations in the Bering Sea, 14 stations in the Chukchi Sea, and 6 stations in the Canadian Basin. Water samples were collected at two depths with a rosette sampler equipped

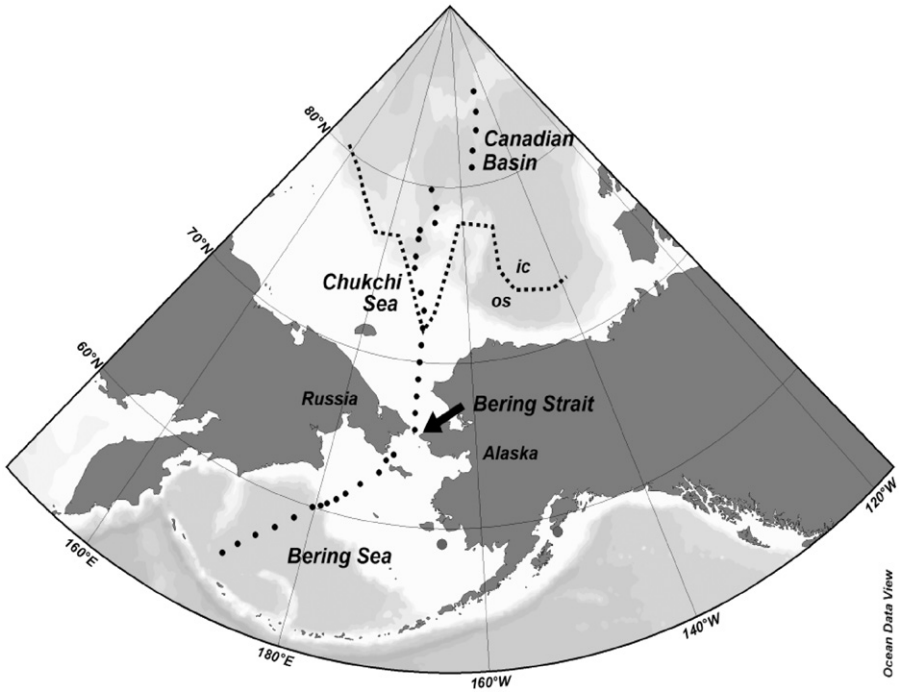

Fig. 1. Locations of sampling stations in the Arctic Sea visited from 19 July to 5 September 2008. op: open waters; ic: ice-covered. Four oceanographic provinces were identified: Bering Sea (stations BR23 to NB21), Bering Strait (stations BS01 to R01), Chukchi Sea (stations R03 to N01), and Canadian Basin (stations D80 to B85).

with 20 L Niskin-type bottles (OceanTest Equipment, Inc., FL, USA), an *in situ* fluorometer (SeaPoint), and a high-precision Sea-Bird *plus* CTD probe. Two depth layers were sampled: at the surface and at the subsurface chlorophyll *a* maximum (SCM) by CTD fluorometry (Thomson and Fine, 2003). The subsurface chlorophyll maximum layer depths were estimated according to Martin et al. (2010). The depth of the SCM was defined as the depth where *in situ* fluorescence measured by CTD was at a maximum, while its thickness was estimated as the zone of elevated fluorescence between areas where the mean vertical

Table 1
Information about the study area in summer 2008 (sea ice cover is provided in percentages; N=no sea ice).

Station	Location		Depth (m)	Sea ice (%)	Station	Location		Depth (m)	Sea ice (%)
	Longitude	Latitude				Longitude	Latitude		
Bering Sea					**Chukchi Sea**				
BR23	169°55.855′E	53°16.079′N	2078	N	R03	169°01.500′W	67°59.200′N	51	N
BR25	171°56.550′E	54°58.432′N	3100	N	R05	168°59.720′W	68°59.700′N	47	N
BR01	173°03.008′E	55°58.279′N	3700	N	R07	168°59.500′W	69°59.700′N	31	N
BR02	174°30.303′E	56°59.873′N	3800	N	R09	168°58.400′W	70°59.600′N	45	N
BR03	176°13.844′E	57°57.877′N	3780	N	R11	168°58.111′W	71°59.426′N	46	70
BR04	177°55.868′E	58°59.645′N	3720	N	R13	169°00.000′W	73°00.000′N	72	20
BR06	179°40.897′E	60°00.250′N	2680	N	R15	169°60.400′W	73°59.500′N	175	N
BR08	179°25.291′W	60°14.592′N	929	N	M06	172°00.000′W	75°20.200′N	846	0
BR10	178°45.875′W	60°30.508′N	240	N	M04	172°06.291′W	75°59.979′N	2020	5
BR12	177°45.478′W	60°54.903′N	138	N	M02	172°03.420′W	76°59.737′N	2300	30
BR13	176°48.540′W	61°23.914′N	108	N	M01	171°59.552′W	77°30.275′N	2280	10
BR15	175°14.825′W	62°11.934′N	227	N	P31	168°00.716′W	77°59.864′N	433	5
NB22	173°07.117′W	63°06.897′N	63	N	N03	167°53.448′W	78°50.380′N	2654	10
NB21	172°25.034′W	63°56.563′N	50	N	N01	170°00.020′W	79°49.960′N	3340	90
Bering Strait					**Canadian Basin**				
BS01	171°28.188′W	64°20.344′N	42	N	D80	158°02.970′W	80°02.080′N	3711	10
BS12	168°51.921′W	65°59.971′N	47	N	D81	155°17.580′W	81°02.070′N	3846	90
R01	169°00.100′W	66°59.466′N	42	N	D82	154°10.380′W	81°56.040′N	3232	30
					D83	150°57.870′W	83°00.660′N	3157	10
					D84	148°45.920′W	83°59.820′N	2490	20
					B85	147°03.360′W	85°07.830′N	2078	99

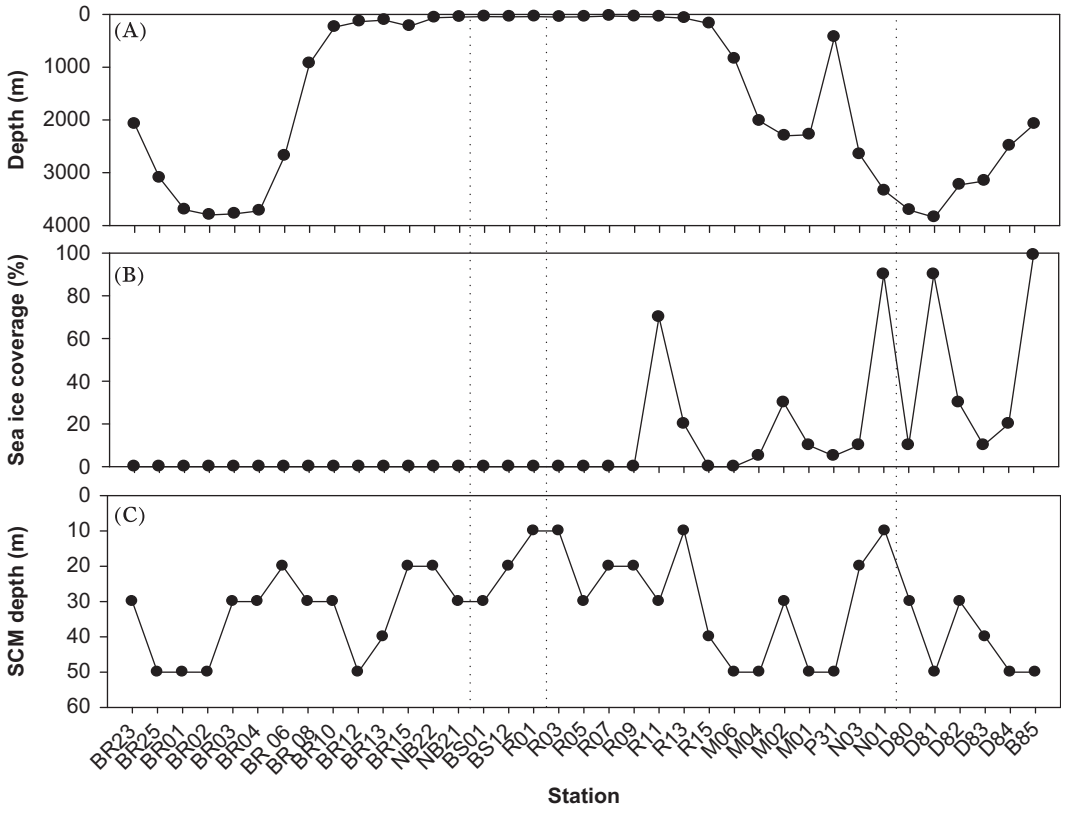

Fig. 2. Variations of water depth (A), sea ice coverage (B), and depths of the chlorophyll *a* maximum—SCM (C) along a transect across the study area. All stations are plotted against longitude (from low latitudes (left) to high latitudes (right)); Bering Sea (stations BR23 to NB21), Bering Strait (stations BS01 to R01), Chukchi Sea (stations R03 to N01), and Canadian Basin (stations D80 to B85).

gradient of *in situ* fluorescence (d(*in vivo* fluorescence)/d*z*) was zero over 5 consecutive depth layers. The ice coverage was visually estimated from the bridge of R.V. *Xuelong*.

2.2. Temperature and salinity—CTD

The hydrographic characteristics and fluorescence profiles of the sampled stations were determined by CTD casts made with a Sea-Bird 911plus system (Sea-Bird, Inc., NY, USA). The CTD fluorometer was calibrated against the chlorophyll *a* (Chl *a*) concentration. A quadratic polynomial equation was used to calibrate fluorometer data against extracted chlorophyll *a* measurements (Parsons et al., 1984) from discrete water samples.

2.3. Sample collection: HPMA slides

Water samples were obtained with a CTD/rosette unit in 20 L PVC Niskin bottles during the 'up' casts. Aliquots of 125 mL were preserved with glutaraldehyde (final concentration 1%). Sample volumes of 50–100 mL were filtered through Gelman GN-6 Metricel filters (0.45 μm pore size, 25 mm diameter; Gelman Sciences, Inc., NY, USA). The filters were mounted on microscopic slides in a water-soluble embedding medium (HPMA, 2-hydroxypropyl methacrylate) on board. The HPMA slides were used for identification and estimation of cell concentration and biovolume. The HPMA-mounting technique, first described by Crumpton (1987), has some advantages over the classical Utermöhl sedimentation method (Kang et al., 1993b). Samples were also collected via phytoplankton net tows (20 μm mesh) and preserved with glutaraldehyde (final concentration 2%); these samples were used only for identification of small species in the phytoplankton assemblage. Since the results from this can be biased towards larger specimens, these data were not used for statistical analysis, but only for morphological and systematic analysis.

2.4. Identification, counts, and biovolume of phytoplankton

Identification by light microscopy is time-consuming and requires a high level of taxonomic skills, but it is still the most reliable method of microalgal identification (Tomas, 1997; Bérard-Therriault et al., 1999). Therefore, at least 300 cells were identified from each sample using a microscope (BX51, Olympus, Inc., Tokyo, Japan), with a combination of light and epifluorescence microscopy at 400× for microplankton, and at 1000× for autotrophic pico- and nanoplankton (Booth, 1993). For species that could not be identified with light microscopy, a JEOL JSM-5600LV scanning electron microscope (JEOL, Inc., Tokyo, Japan) was used. Autotrophic pico- and nanoflagellates were filtered, dehydrated, and dried according to methods described by Jung et al. (2009). Whole mounts coated with graphite and gold were used for SEM analysis. Cell counts were converted to cell concentrations as described by Kang and Fryxell (1991) and Kang et al. (1993a). Cell dimensions of dominant phytoplankton species were measured to the nearest 1 μm for subsequent estimations of biovolume using appropriate geometric shapes (Sun and Liu, 2003; Strathmann, 1967). Linear dimensions were measured by light microscopy (BX51, Olympus) and SEM (JSM-5600LV, JEOL). Twenty or more individual cells were measured to avoid biasing results. The information on taxa and linear dimensions were then

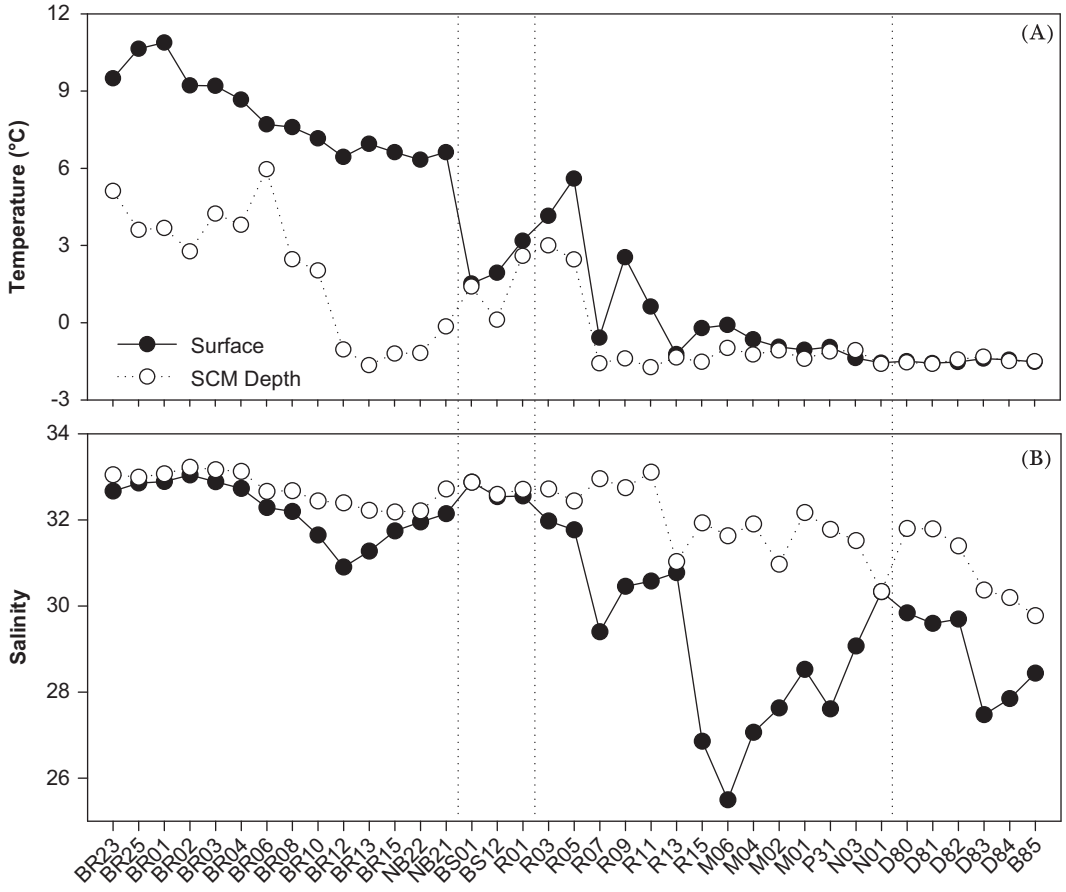

Fig. 3. Distribution of the water temperature (A) and salinity (B) at surface and SCM depth according to latitude (from low latitudes (left) to high latitudes (right); Bering Sea (stations BR23 to NB21), Bering Strait (stations BS01 to R01), Chukchi Sea (stations R03 to N01), and Canadian Basin (stations D80 to B85)).

transferred to a Microsoft Excel worksheet and biovolume was calculated according to Sun and Liu (2003)—see also Menden-Deuer and Lessard (2000).

2.5. Statistical analysis

A non-metric cluster analysis was used in conjunction with the Bray–Curtis similarity index after logarithmic transformation of species biovolume data. Significance levels of differences among stations for the phytoplankton assemblages were obtained using the similarity programs ANOSIM and SIMPER of the Plymouth Routine In Multivariate Ecological Research (PRIMER, version IV; Clarke and Warwick, 1994) software package: cluster analysis was performed using group average clustering from Bray–Curtis similarities. Using the ranked similarity matrix, an ordination plot was produced by non-metric multidimensional scaling (MDS) (see Sokal and Rohlf, 1995).

The Shannon–Wiener diversity index was used to analyze species diversity, and Pielou's evenness was used to measure the relative abundance of species at each station. To estimate the relationships between phytoplankton abundance and temperature and salinity, the Pearson's product moment correlation was used. For each sampling date the average abundance of species over all sampling stations was used to calculate the diversity indices.

3. Results and discussion

Information about the study area is provided in Table 1. The sampling stations in the Arctic Ocean were visited from 19 July to

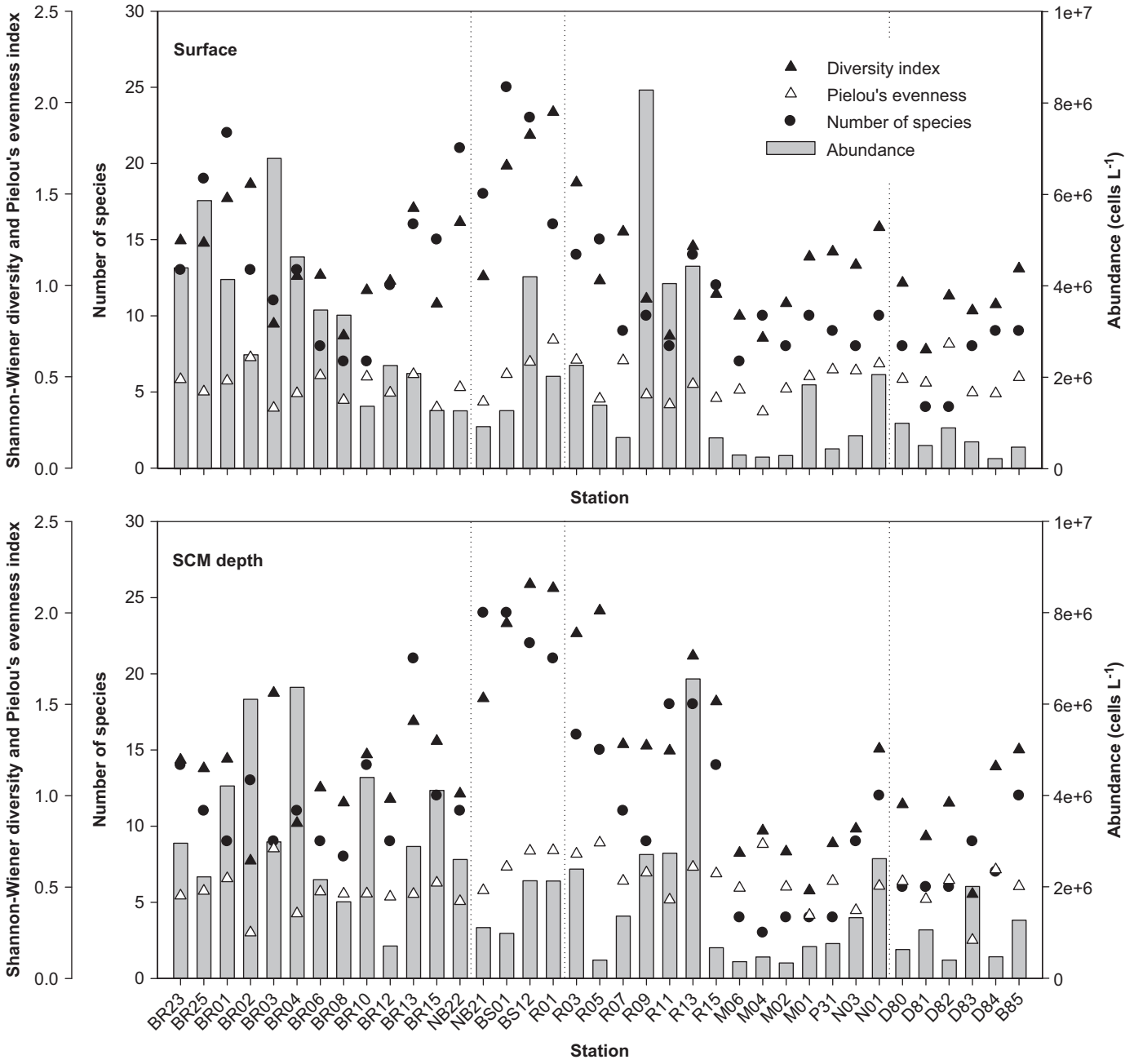

Fig. 4. Shannon–Wiener diversity, evenness, number of species, and abundance of a group of unidentified pico-nano size phytoplankton according to latitude (from low latitudes (left) to high latitudes (right); Bering Sea (stations BR23 to NB21), Bering Strait (stations BS01 to R01), Chukchi Sea (stations R03 to N01), and Canadian Basin (stations D80 to B85)).

Table 2
Phytoplankton species (cell abundance, cells L^{-1}) recorded during summer sampling, grouped by latitude in the Western Arctic sea (Sur.: surface, SCM: depth of chlorophyll *a* maximum; BR: Bering Sea, BS: Bering Strait, CS: Chukchi Sea, CB: Canadian Basin, and ND: not detected).

	BR		BS		CS		CB	
	Sur.	**SCM**	**Sur.**	**SCM**	**Sur.**	**SCM**	**Sur.**	**SCM**
Dinophyceae	ND	ND	ND	ND	ND	ND	ND	ND
Alexandrium sp.	ND	ND	ND	ND	2.80E+02	ND	ND	ND
Ceratium carriense	ND	ND	ND	ND	ND	ND	3.00E+01	ND
Ce. focus	4.00E+01	ND	ND	ND	ND	ND	ND	ND
Ce. horridum	4.00E+01	ND	ND	ND	ND	ND	ND	1.00E+01
Ce. lineatum	1.04E+03	ND	ND	ND	2.00E+02	ND	ND	ND
Ce. longipes	ND	3.00E+01	ND	ND	ND	ND	ND	ND
Ce. pentagonum	ND	ND	ND	ND	4.00E+01	ND	ND	ND
Ce. tripos	5.80E+02	ND	4.00E+01	ND	8.00E+01	ND	ND	ND
Ceratium sp.	ND	ND	ND	ND	ND	1.00E+01	ND	1.00E+01
Dinophysis norregica	1.80E+02	ND	ND	ND	8.00E+01	ND	ND	ND
Gymnodinium arcticum	1.93E+04	ND	ND	ND	ND	ND	ND	ND
Gymnodinium. sp.	8.14E+03	1.23E+04	ND	ND	7.80E+02	1.00E+05	2.20E+04	2.50E+04
Gyrodinium sp.	ND	1.92E+03	ND	3.00E+01	ND	3.40E+02	4.39E+02	ND
Heterocapsa sp.	ND	ND	ND	ND	8.80E+03	4.39E+02	1.32E+03	7.02E+03
Phalacroma sp.	1.76E+03	ND	ND	ND	ND	ND	ND	ND
Prorocentrum sp.	ND	6.00E+01	ND	ND	ND	ND	ND	ND
Protoperidinium sp.	2.60E+02	8.00E+01	ND	ND	3.40E+02	ND	ND	ND
Bacillariophyceae	ND	ND	ND	ND	ND	ND	ND	ND
Achnanthes sp.	ND	ND	ND	ND	ND	ND	ND	ND
Actinocyclus actinochilus	ND	ND	ND	ND	4.39E+04	1.84E+04	ND	ND
Actynocyclus sp.	ND	8.88E+02	ND	ND	1.40E+04	ND	ND	5.27E+03
Asteromphalus sp.	1.78E+03	ND	1.08E+03	ND	ND	4.39E+02	ND	ND
Bacteriastrum sp.	2.00E+01	ND	ND	ND	ND	ND	ND	ND
Chaetoceros affinis	1.18E+03	5.75E+04	4.24E+03	9.66E+03	ND	7.37E+04	ND	ND
Ch. atlanticus	ND	3.34E+04	ND	ND	ND	ND	ND	ND
Ch. compressus	1.17E+05	4.48E+04	1.34E+04	4.39E+04	ND	5.74E+05	ND	1.05E+04
Chaetoceros concavicornis	4.78E+03	1.05E+04	8.31E+03	6.41E+04	1.80E+02	5.27E+04	ND	ND
Ch. convolutes	6.20E+02	6.11E+04	1.18E+03	ND	ND	7.55E+04	ND	ND
Ch. curvicetus	1.00E+03	ND	ND	4.57E+04	2.60E+02	ND	ND	ND
Ch. danicus	ND	ND	ND	ND	4.00E+01	ND	ND	ND
Ch. debilis	3.58E+03	1.48E+05	4.45E+04	5.27E+03	ND	1.00E+05	ND	ND
Ch. decipiens	5.60E+02	3.69E+04	2.30E+04	5.27E+03	1.76E+03	ND	1.32E+03	ND
Ch. diadema	2.80E+02	8.78E+02	1.00E+03	1.04E+05	ND	1.27E+04	ND	ND
Ch. didymus	ND	ND	1.34E+03	ND	ND	ND	ND	ND
Ch. furcellatus	ND	4.92E+04	ND	8.78E+04	ND	ND	ND	ND
Ch. lorenzianus	5.27E+03	3.07E+03	ND	3.16E+04	ND	2.11E+04	ND	ND
Ch. mitra	5.80E+02	ND	ND	ND	4.60E+02	ND	ND	ND
Ch. peruvianus	1.54E+03	4.39E+02	ND	ND	4.00E+01	1.54E+04	ND	ND
Ch. simplex	ND	ND	6.80E+05	ND	ND	ND	ND	ND
Ch. socialis	ND	ND	ND	ND	ND	1.94E+05	ND	7.02E+03
Chaetoceros sp.	1.54E+04	1.21E+05	6.51E+04	1.10E+05	1.20E+03	2.24E+06	3.25E+04	8.78E+03
Coconeis sp.	ND	ND	ND	ND	ND	5.27E+03	ND	ND
Corethron criophilum	1.20E+02	1.00E+01	ND	ND	ND	ND	ND	ND
Cosinodiscus sp.	ND	4.00E+01	ND	1.40E+02	2.80E+02	2.80E+02	ND	ND
Cylindrotheca sp.	7.99E+04	1.12E+06	3.95E+04	3.40E+05	4.61E+05	1.89E+06	ND	ND
Detonula confervacea	4.54E+03	3.50E+03	ND	4.90E+02	ND	ND	ND	ND
Diploneis sp.	1.96E+04	ND	ND	ND	ND	ND	ND	ND
Fragilariopsis sp. (>20 μm)	6.59E+04	2.16E+05	3.80E+04	ND	2.02E+05	7.33E+05	ND	ND
Fragilariopsis sp. (<20 μm)	1.90E+06	9.44E+05	3.51E+03	ND	1.54E+05	3.29E+04	3.07E+03	2.19E+04
Fragilaria striatula	ND	1.11E+05	ND	ND	ND	ND	ND	ND
Fragilaria sp.	2.28E+04	4.27E+03	1.70E+05	1.56E+05	6.57E+05	6.84E+05	ND	ND
Leptocylindrus sp.	ND	ND	ND	4.39E+04	ND	ND	ND	ND
Melosira sp.	ND	ND	ND	2.80E+02	ND	ND	ND	ND
Minidiscuss sp.	8.78E+04	1.10E+05	ND	8.78E+04	1.10E+05	2.19E+04	ND	5.49E+04
Neodentculata seminae	5.27E+03	ND	ND	ND	ND	ND	ND	ND
Navicula transitans var. *derasa*	ND	ND	ND	ND	ND	ND	ND	ND
Navicula sp.	4.43E+04	9.98E+02	1.23E+04	4.83E+04	3.30E+04	2.11E+04	ND	1.32E+05
Nitzschia sp.	5.14E+04	3.07E+05	1.58E+04	2.73E+05	4.17E+05	6.32E+04	ND	1.10E+04
Paralia sulcata	ND	ND	ND	2.60E+02	ND	1.76E+03	ND	ND
Pleurosigma sp.	ND	ND	ND	ND	6.00E+01	1.45E+04	ND	ND
Pseudonitschia seriata	ND	1.45E+04	ND	ND	ND	6.15E+04	ND	ND
Pseudonitschia. sp.	2.21E+05	5.89E+03	6.03E+04	7.00E+01	3.69E+04	2.37E+04	ND	ND
Rhizosolenia hebatata	ND	4.00E+01	ND	1.10E+02	ND	ND	ND	ND
Rhizosolenia sp.	7.00E+02	7.00E+01	6.00E+02	2.60E+02	2.40E+02	7.00E+01	5.00E+01	ND
Thalassionema javanicum	2.00E+01	ND	ND	ND	ND	ND	ND	ND
Thalassionema sp.	ND	2.30E+02	1.06E+04	ND	ND	ND	ND	ND
Thalassiosira antartica	ND	1.22E+04	1.95E+05	7.02E+03	ND	1.36E+04	ND	ND
Th. australes	ND	1.67E+04	ND	ND	ND	ND	ND	ND
Th. baltica	ND	ND	9.07E+04	ND	ND	ND	ND	ND
Th. bulbosa	ND	5.71E+03	ND	1.05E+04	ND	2.77E+04	ND	ND

Table 2 (*continued*)

	BR		BS		CS		CB	
	Sur.	**SCM**	**Sur.**	**SCM**	**Sur.**	**SCM**	**Sur.**	**SCM**
Th. delicatula	ND	1.32E+03	ND	ND	1.23E+04	ND	ND	ND
Th. eccentric	ND	2.33E+04	1.02E+05	4.21E+04	ND	2.85E+04	ND	ND
Th. gravid	ND	ND	6.15E+04	4.57E+04	ND	ND	ND	ND
Th. nordenskioldii	ND	3.51E+04	6.05E+05	2.44E+05	2.00E+05	6.76E+04	ND	ND
Th. pacifica	ND	6.58E+03	ND	7.02E+04	ND	ND	ND	ND
Th. simonsenii	3.20E+02	ND	ND	2.28E+04	ND	ND	ND	ND
Thalassiosira sp. (>200 μm)	2.00E+01	ND	ND	ND	ND	ND	ND	ND
Thalassiosira sp. (>20 μm, <200 μm)	2.86E+04	4.05E+04	2.42E+05	1.23E+05	9.72E+04	8.87E+04	ND	1.76E+03
Thalassiosira sp. (<20 μm)	ND	ND	ND	ND	ND	ND	2.63E+03	ND
Thalassiothrix sp.	7.00E+02	ND	1.00E+02	1.00E+02	4.00E+01	ND	ND	ND
Cryptophyceae	ND	ND	ND	ND	ND	ND	ND	ND
Cryptomonas sp.	1.68E+06	3.07E+06	4.39E+04	6.58E+04	3.51E+05	6.04E+05	ND	9.88E+04
Chrysophyceae	ND	ND	ND	ND	ND	ND	ND	ND
Dinobryon belgica	9.87E+05	2.62E+06	ND	ND	1.73E+05	1.40E+04	3.56E+04	ND
Dictyochophyceae	ND	ND	ND	ND	ND	ND	ND	ND
Dictyocha speculum	2.00E+01	1.40E+03	ND	ND	4.58E+04	7.46E+03	1.32E+03	3.51E+03
D. speculum var. *speculum*	ND	ND	ND	ND	ND	2.55E+04	ND	1.67E+04
Meringosphaera mediterranea	5.27E+03	ND	ND	ND	5.47E+03	3.51E+03	8.34E+03	1.32E+04
Prasinophyceae	ND	ND	ND	ND	ND	ND	ND	ND
Halosphaera sp.	ND	8.78E+02	ND	ND	ND	ND	2.63E+05	ND
Pyramimonas sp.	5.93E+05	4.39E+05	7.68E+04	ND	3.29E+04	ND	7.68E+04	9.88E+04
Prymnesiophyceae	ND	ND	ND	ND	ND	ND	ND	ND
Phaeocystis sp.	1.59E+06	8.45E+05	2.19E+06	3.51E+05	1.27E+06	1.24E+06	ND	ND
unidentified sp. (micro size)	1.64E+03	1.00E+01	1.12E+03	ND	9.40E+02	ND	1.40E+02	ND
unidentified sp. (nano size)	1.56E+07	1.21E+07	1.26E+06	1.78E+06	1.25E+07	8.33E+06	1.04E+06	1.72E+06
unidentified sp. (pico size)	2.12E+07	2.18E+07	1.42E+06	1.02E+06	1.09E+07	5.87E+06	2.17E+06	3.59E+06

5 September 2008. Four oceanographic provinces were identified: the Bering Sea (stations BR23 to NB21), the Bering Strait (stations BS21 to R01), the Chukchi Sea (stations R03 to N01), and the Canadian Basin (stations D80 to B85) (Fig. 1).

3.1. Sea ice coverage

Visual observations of ice conditions were conducted at each sampling station. Visual estimates of sea ice coverage were done at several stations during summer 2008 (Table 1). Sea ice was composed of large continuous ice sheets on the shelf (Northern Bering Sea, Bering Strait, and Southern Chukchi Sea). Here, less than 40% of the visible area around the sampling site was ice-covered (8 stations in the Chukchi Sea and all stations in the Canadian Basin). In the northern Chukchi Sea, ice cover consisted of highly fragmented and partly submerged floes, which covered roughly 30% of the surface area in the northern Chukchi Sea. In the Canadian Basin, ice covered about 40% of the sea surface.

It is difficult to estimate the overall amount of light that was received by different water masses in the area due to constantly shifting ice floes and sea ice coverage. It is reasonable to assume that during summer, the water column has been exposed to higher irradiance due to a lower ice cover, both in terms of area covered by annual ice and in terms of ice thickness. Sea ice absorbs and reflects sunlight. Several studies, including Hill et al. (2005), observed chlorophyll concentrations characteristic of bloom conditions in regions along the ice edge that were highly dominated by small prasinophytes and larger haptophytes and diatoms. We did not study the particular situation along the annual or multiannual ice edge. However, in the pack ice covered Chukchi Sea (Fig. 2) we found a higher proportion of smaller cells at surface and SCM depth. In the Canadian Basin, populations were dominated by smaller microalgae that showed indications of low light adaptation. This can best be explained by low nutrient levels and a long period of ice cover that prevented larger cells from growth and photosynthetic production.

3.2. Temperature and salinity

Distributions of water temperature and salinity varied by latitude from 10.9 to 1.6 °C and 33.0–25.4 at surface, and 6.0–1.7 °C and 33.2–29.7 at SCM depth (Fig. 3). Water temperature was lower at higher latitude with sea ice cover. Salinity showed a pattern similar to water temperature.

Water temperature was the environmental parameter that correlated with phytoplankton abundance along our latitudinal transect in the Bering Sea (surface, Pearson's correlation coefficient $r=0.785$, $n=14$) where phytoplankton abundance increased with water temperature within the euphotic zone. This positive correlation is corroborated by published records from the Arctic Ocean (Sukhanova et al., 2009). Given the transition towards a new, warmer state in the course of climate change (Lassen et al., 2010), it is expected that the relative abundance of picophytoplankton will increase, whereas larger phytoplankton will decrease in Arctic regions, since smaller phytoplankton are characteristic for temperate or warmer oceans (Lassen et al., 2010). In fact, Li et al. (2009) reported recently that small phytoplankton thrive but large phytoplankton languish under changing environmental conditions in the Arctic Ocean.

In the western Arctic, warm Pacific waters from the south determine the timing of the seasonal ice melting in spring, as well as the timing of ice formation in fall (Coachman et al., 1975). Inflow of warm water masses through the Bering Strait and seasonally variable environmental factors provide great spatial and temporal variability of the physical oceanographic features in the western Arctic (Weingartner et al., 2005; Carmack and Wassmann, 2006). High fluctuations of temperature occur in the Bering Strait due to the effects of the three currents: Anadyr water, Alaska coastal water, and Bering Strait shelf water

(Grebmeier et al., 2006a). This variability may affect the systematic composition, abundance, and biomass of phytoplankton, as well as phytoplankton succession and primary productivity, as suggested before by Hill and Cota (2005).

Hill et al. (2005) found stratification of the surface waters in summer in the area due to a lowering of surface salinity to 24–29 from the melting of sea ice, and temperatures reach as high as +0.25 °C with solar heating of the water column after ice melted away. Temperatures showed a similar range between the surface and subsurface in this study, whereas salinity (*S*) in the euphotic zone ranged between 29.0 and 34.0, and temperature (*T*) ranged between 1.9 and 1.3 °C in summer (Fig. 3). In the Bering Strait, the surface temperature went down suddenly since surface and subsurface layers were well mixed in this area. The lowest salinity was found in middle of the Canadian Basin (subsurface depth at station M06), which might be due to melting sea ice. According to

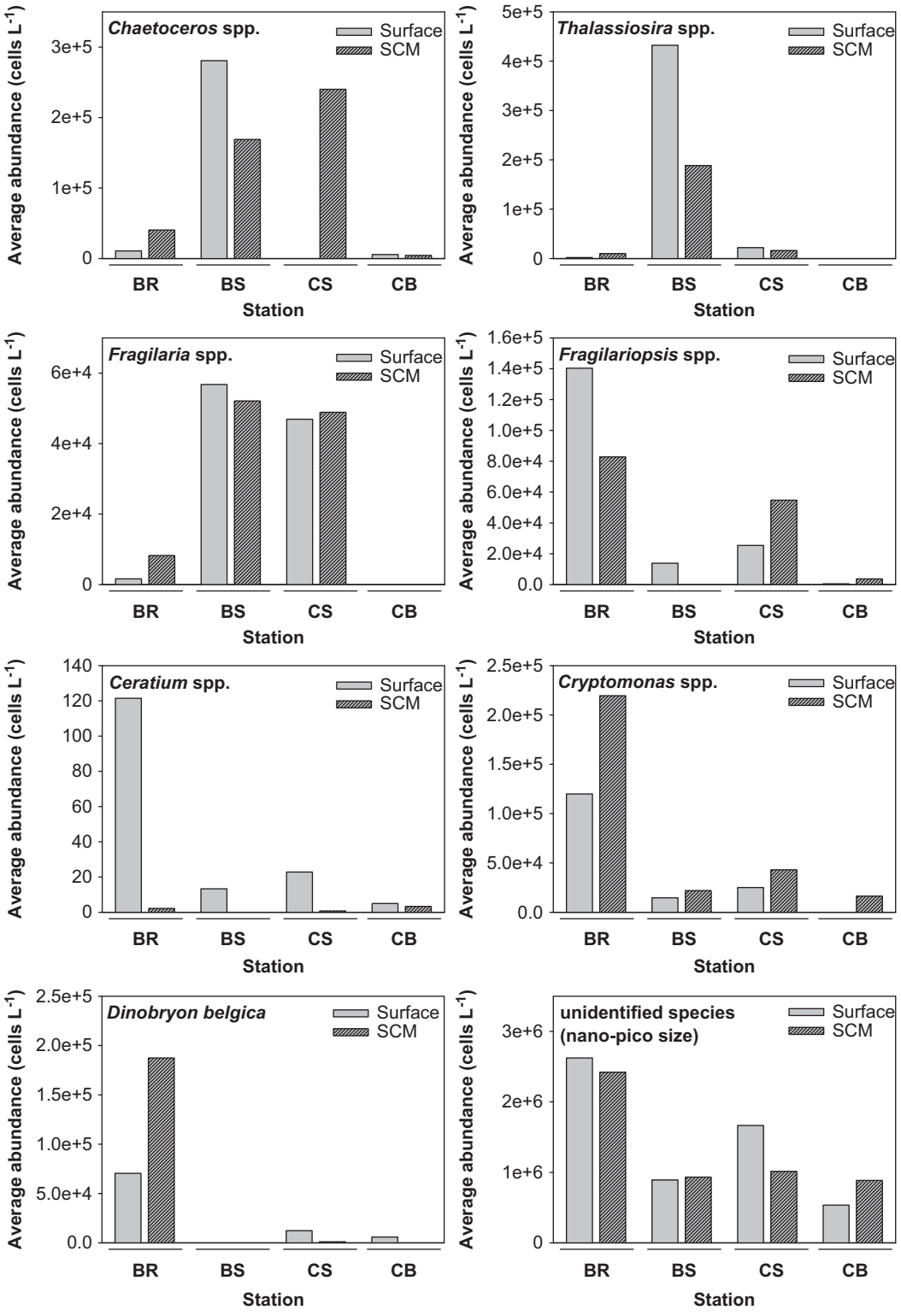

Fig. 5. Average abundance of major dominant species in the study area (BR: Bering Sea, BS: Bering Strait, CS: Chukchi Sea, and CB: Canadian Basin).

Hill et al. (2005), shelf stations in their study showed slightly higher salinity and lower temperature compared to situations on the slope and the Canadian Basin in spring.

3.3. Subsurface chlorophyll a maximum—SCM

Variations of the depths of the SCM along the study area transect are provided in Fig. 2(C). Here, all stations are plotted against latitude. The vertical distribution of microalgal assemblages shows a similarity between surface and subsurface communities. Both depth layers show remarkable fluctuations along the whole transect (Fig. 4). However, the taxon composition differs between surface and the SCM (Table 2). Here, Prymnesiophyceae (for example the dominant *Pyramimonas* sp.) showed a higher abundance at the surface than at the SCM. We found slightly higher abundances in terms of cell numbers at the surface compared to the SCM (not considering

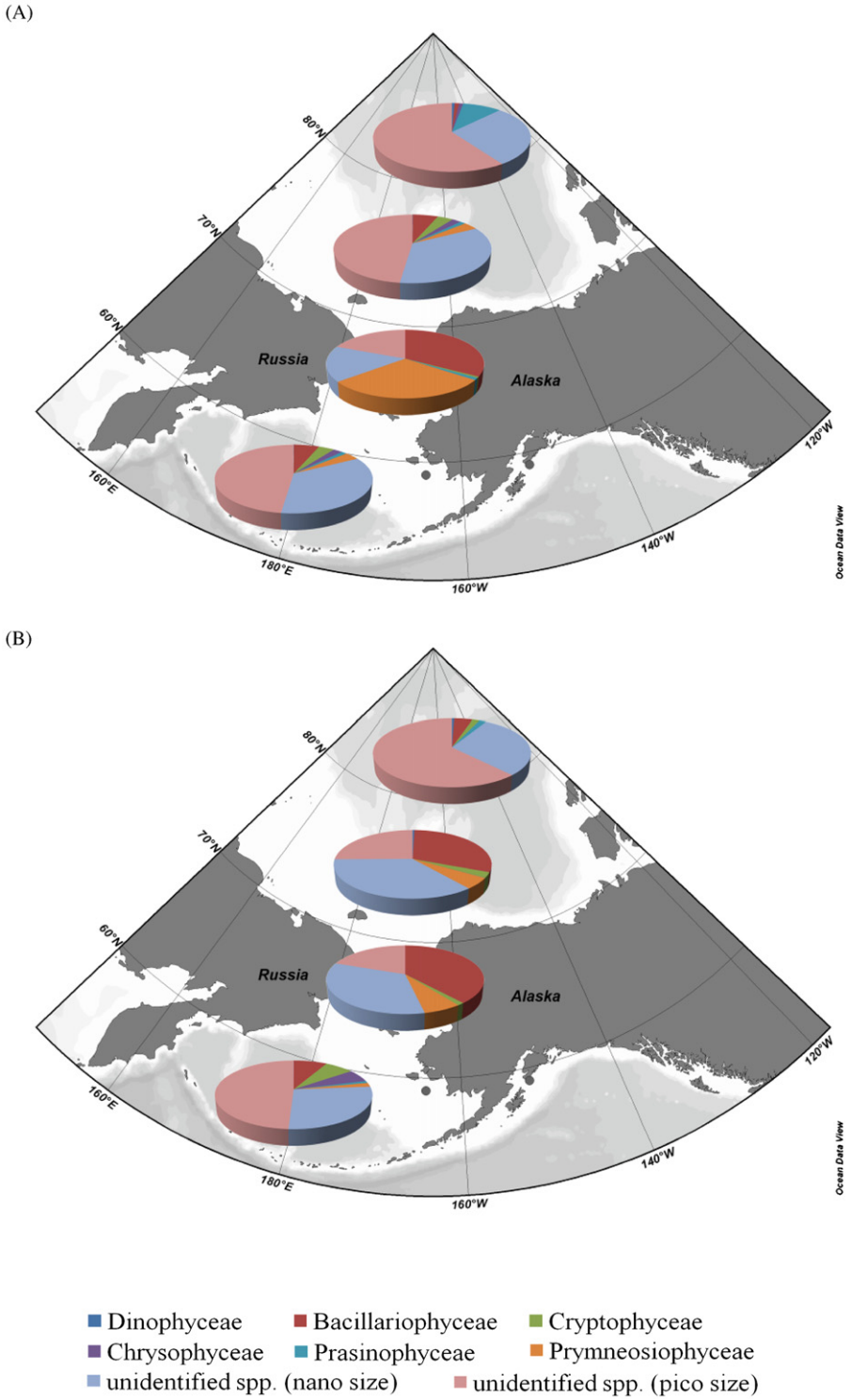

Fig. 6. Composition of phytoplankton communities by abundance in the study area (A: surface, B: SCM depth). The pie chart shows relative abundances of the major taxa: Dinophyceae, Bacillariophyceae, Cryptophyceae, Chrysophyceae, Prasinophyceae, Prymnesiophyceae, unidentified nano-sized phytoplankton, and unidentified pico-sized phytoplankton.

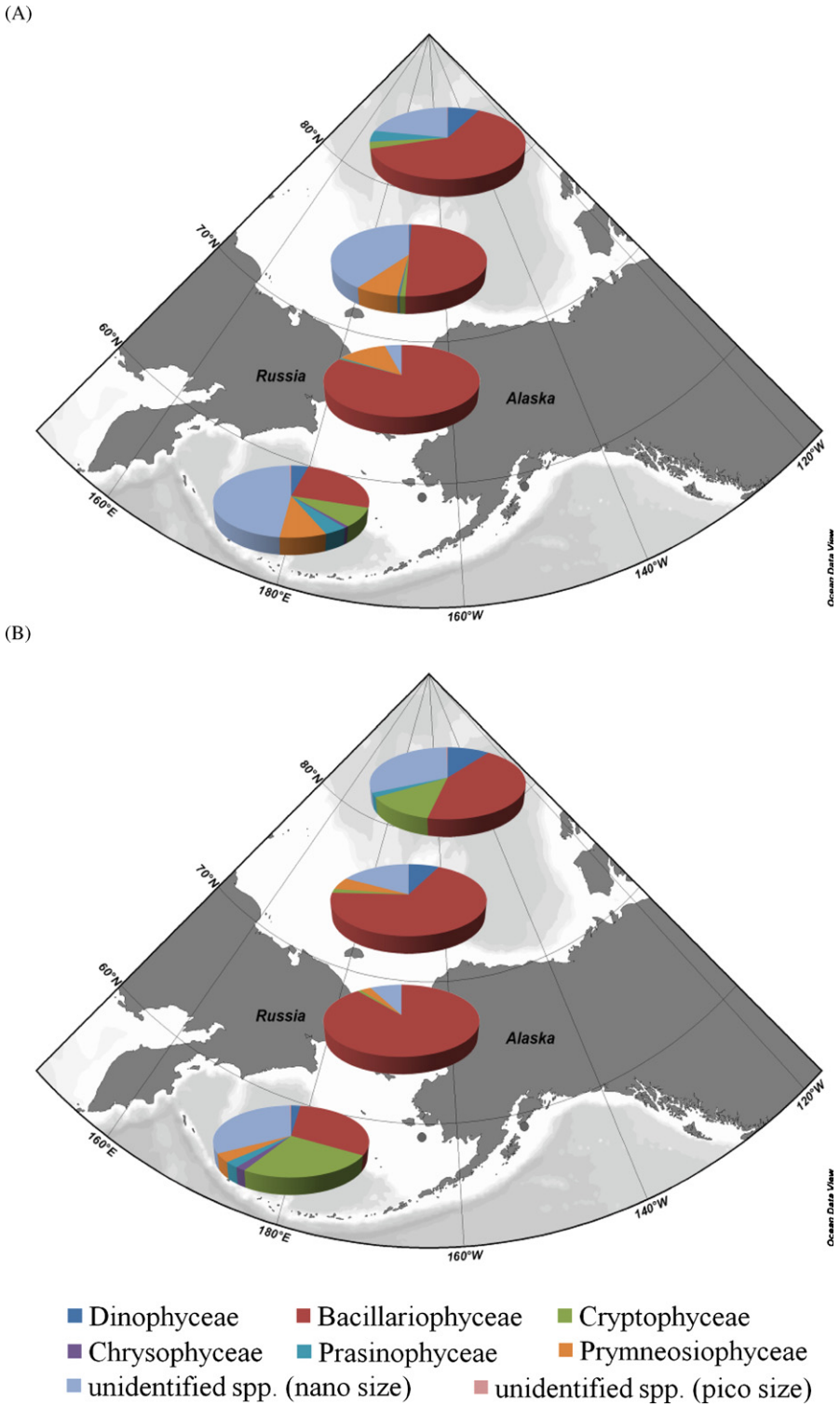

Fig. 7. Composition of phytoplankton communities by biomass in the study (A: surface, B: SCM depth). The pie chart shows relative abundances of the major taxa: Dinophyceae, Bacillariophyceae, Cryptophyceae, Chrysophyceae, Prasinophyceae, Prymnesiophyceae, unidentified nano-sized phytoplankton, and unidentified pico-sized phytoplankton.

the northern Chukchi Sea, where generally low abundances did not permit a meaningful comparison). This is corroborated by Sukhanova et al. (2009), who found the highest concentration of cells in the surface layer of the western Arctic. In their study highest phytoplankton abundances were between the surface layer and a depth of 16 m. There were striking differences in the vertical distribution of dominant taxa. In the upper layer, the diatom *Pauliella taeniata* provided 65% of the total abundance, whereas in the lower layer, the genus *Thalassiosira* provided 65% of the abundance. *Thalassiosira* spp. provides a biomass of 50% in the upper and 83% in the deeper layers of the western Arctic (Sukhanova et al., 2009). At the margin of the observed bloom, the authors found maximum diatom abundances in the lower portion of the euphotic zone where *P. taeniata*, *F. oceanica*, and *Melosira* sp. dominated.

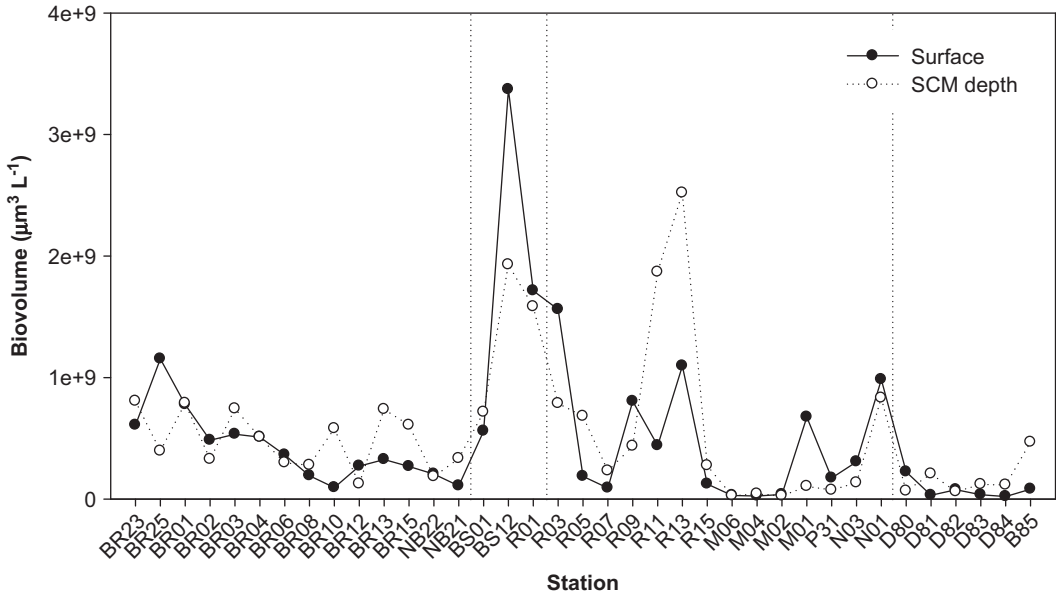

Fig. 8. Distribution of phytoplankton biomass ($\mu m^3\ L^{-1}$) with respect to the latitudinal sequence of stations (from low latitudes (left) to high latitudes (right); Bering Sea (stations BR23 to NB21), Bering Strait (stations BS01 to R01), Chukchi Sea (stations R03 to N01), and Canadian Basin (stations D80 to B85)).

We did not find any dominance with depth of these 3 taxa. *P. taeniata* was not found during our investigation either. This difference might be due to the different study sites between studies. Their study site was situated east of our transect. However, the reason for this depth difference remains to be discovered.

3.4. Phytoplankton abundance, biovolume, and size

The average abundance of the major dominant species in the study area shows an interesting pattern (Fig. 5). The major dominant diatom species were distributed in the Bering Strait and the southern Chukchi Sea, except for *Fragilariopsis* spp., since this area represents a mixed area where 3 currents concatenate. However, flagellates (e.g. *Ceratium* sp., *Cryptomonas* spp., and *Dinobryon belgica*) showed high abundances in the Bering Sea. In the Bering Sea, phytoplankton abundances decreased towards the Bering Strait in the north, both at the surface and at the SCM. Despite the lack of high abundances in the Bering Strait, this area shows the highest biovolume since large diatom cells were dominant. There was high phytoplankton abundance in the central Chukchi Sea. The composition of phytoplankton communities by abundance in the study area varied with surface and the SCM depth. A pie chart shows the relative abundance of the following major taxa: Dinophyceae, Bacillariophyceae, Cryptophyceae, Chrysophyceae, Prasinophyceae, Prymnesiophyceae, unidentified pico-sized phytoplankton, and unidentified nano-sized phytoplankton (Fig. 6). The phytoplankton at both depth layers (surface, SCM depth) followed a similar trend for the major taxa mentioned above in terms of their relative biovolume (Fig. 7). Pico-sized plankton has a high ratio in terms of cell number (abundance) in the study area (surface 42.9%, SCM 41.0%). However, the biovolume of pico-sized plankton is smaller in the study area (surface 0.2%, SCM 0.3%), and diatoms contribute primarily to the primary productivity in the study area.

The distribution of phytoplankton biovolume demonstrated a decrease from lower to higher latitudes (Fig. 8). According to Sukhanova et al. (2009) diatoms exceeded 80% of the total phytoplankton abundance and biomass at all stations in the western Arctic (Chukchi Sea and eastern Beaufort Sea). Beyond 50 m water depth in the Chukchi Sea and 200 m in the Beaufort Sea, diatom abundances ranged from tens to thousands of cells per liter (Sukhanova et al., 2009). In our study, the abundance and biovolume of phytoplankton increased and species diversity became richer from the western Bering Sea to the Bering Strait. After passing through the Bering Strait, these parameters decreased, providing a latitudinal gradient towards the central Arctic (Fig. 4).

The most abundant species were of pico-nano ($<20\ \mu m$,) size at the surface and SCM depths at most stations in our study (Table 2). Pico- and nano-sized phytoplankton were abundant in the Bering Sea, whereas diatoms and nano-sized plankton provided the majority of taxon diversity in the Bering Strait and in the Chukchi Sea (Fig. 6). In agreement with comprehensive reviews of the available literature (Agawin et al., 2000; Bell and Kalff, 2001), relatively large phytoplankton ($>2\ \mu m$) were expected to be more abundant in nutrient-rich than nutrient-poor waters, which is corroborated by our investigation (Joo et al., in prep.). But there are other environmental and physiological factors that determine the size structure of phytoplankton, such as temperature (Nona et al., 2000; Behrenfeld et al., 2006) and grazing (Sieburth et al., 1978; Sherr et al., 2003).

3.5. Phytoplankton biodiversity

We recorded phytoplankton species (cell abundance, cells L^{-1}) during our summer sampling according to latitude in the western Arctic Ocean (Table 2). Shannon–Wiener diversity, evenness, number of species, and phytoplankton abundance were analyzed according to latitude (Fig. 4). In our study phytoplankton communities were composed of 71 taxa representing Dinophyceae, Cryptophyceae, Bacillariophyceae, Chrysophyceae, Dictyochophyceae, Prasinophyceae, and Prymnesiophyceae. In the western Arctic (Chukchi Sea and eastern Beaufort Sea), Sukhanova et al. (2009) found representatives of the Pavlovophyceae, Euglenophyceae, Chlorophyceae, Cyanophyceae, and non-identified flagellates. In the Bering Sea, besides the nano- and pico-sized fraction of the phytoplankton, we found the diatom *Fragilariopsis* sp. ($<20\ \mu m$) to be most abundant at the surface (Table 2). *Cryptomonas* sp. (Cryptophyceae) was dominant at the SCM depth. Both *Fragilariopsis* sp. and *Cryptomonas* sp. have larger cells than other dominant species in the area. In the Bering Strait we found *Phaeocystis* sp. (Prymnesiophyceae) at the surface and at

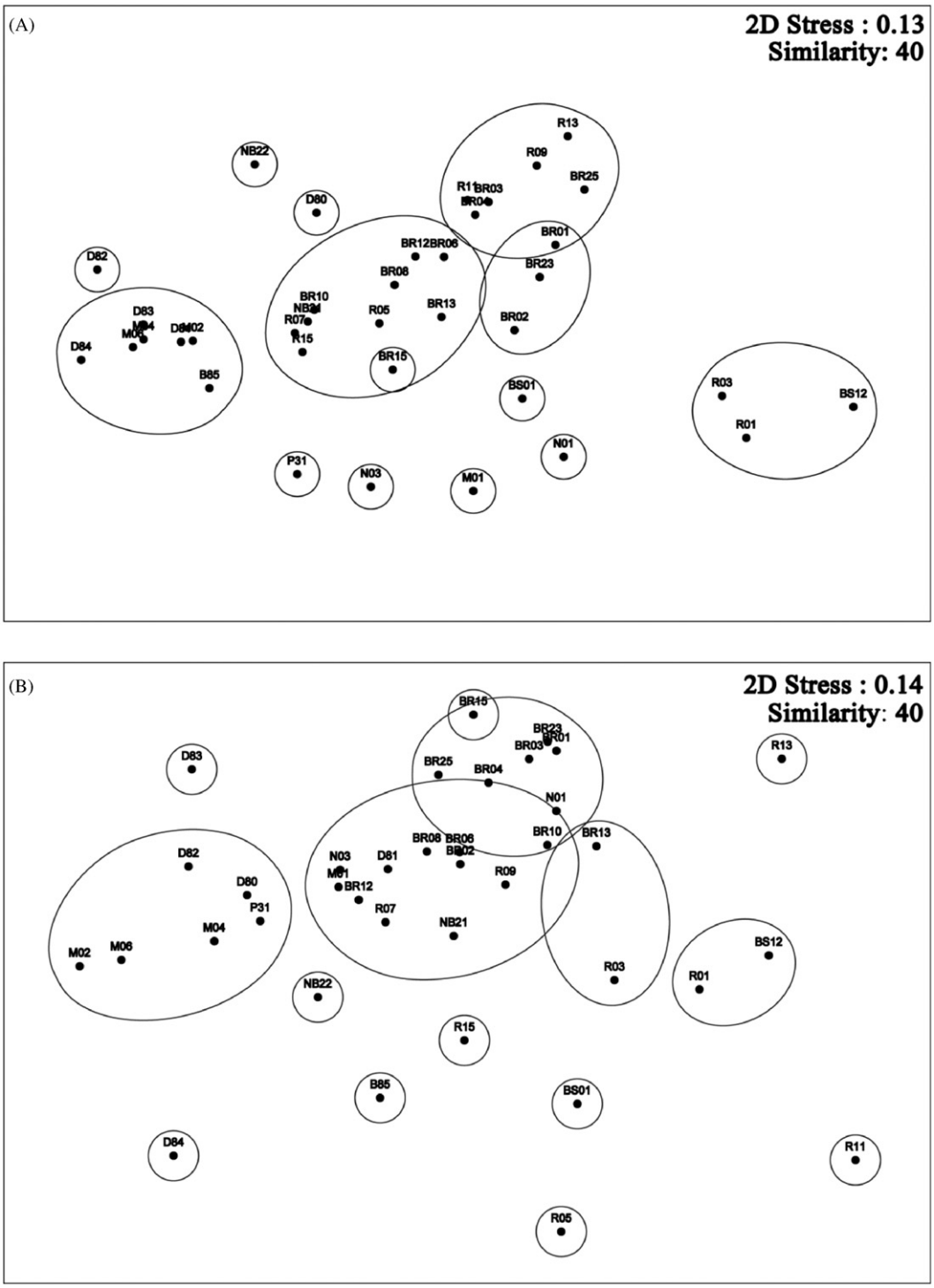

Fig. 9. Two-dimensional MDS configuration with superimposed clusters at Bray–Curtis similarity levels of 40% using biomass ($\mu m^3\ L^{-1}$) water column as factor. Each plot is described by site (A: surface, B: SCM depth).

the SCM depth. In the Chukchi Sea *Phaeocystis* sp. was found to be dominant only at the surface and the diatom *Chaetoceros* sp. was dominant at the subsurface. In the Canadian Basin *Halosphaera* sp. (Prasinophyceae) was dominant at surface, whereas the diatom *Navicula* sp. was dominant at the SCM depth, although in low abundances. These results can be explained by the finding that relatively larger phytoplankton dominate in warmer oceans over smaller phytoplankton (Lassen et al., 2010).

Contrary to our results where *P. taeniata* could not be found at all, Sukhanova et al. (2009) observed that *P. taeniata* was the most dominant diatom species in the Chukchi and eastern Beaufort Seas, comprising up to 95% of the total abundance and up to 85% of the phytoplankton biomass. In addition, we found 7 species of *Thalassiosira* in the Bering Sea not to be remarkably abundant, whereas during a bloom off Point Barrow, *Thalassiosira hyaline*, *Thalassiosira gravida*, *Thalassiosira antarctica*, and *Thalassiosira nordenskioeldii* were dominant in the study of Sukhanova et al. (2009). The latter study took place at the coastal Bering Sea off Point Barrow, though, which is different from our offshore location.

Aizawa et al. (2005) separated the Bering Sea stations into the Aleutian Basin eastern shelf region and the Aleutian Basin. In their study phytoplankton communities on the shelf were dominated by *Thalassiosira* spp. (among others by *T. gravida*, *T. trifulta*, and *T. conferta*), *Chaetoceros debilis* and *Chaetoceros contortus*. Although low in abundance, *Chaetoceros diadema* was generally found on the shelf or close to the Aleutian Islands. The Aleutian Basin assemblage was similar to the shelf assemblage, but the centric diatoms were lower in abundance, while pennate diatoms such as *Pseudo-nitzschia* spp. *Nitzschia seminae*, and *Fragilariopsis pseudonana* dominated in the study of Aizawa et al. (2005). We found that pennate diatoms such as *Fragilariopsis* sp. and pico-nano sized phytoplankton were dominant, while the genera *Chaetoceros* and *Thalassiosira* were rare in the southern Bering Sea (Table 2). This difference might be due to the different study sites between Aizawa's and our study site.

3.6. Latitudinal differences in phytoplankton biovolume

Multidimensional scaling (MDS) analysis was used as a multivariate procedure for detecting natural groupings in the present data. MDS provides a set of related statistical techniques often used in the visualization of data and to explore similarities or dissimilarities in data. MDS is a special case of ordination. An MDS algorithm starts with a matrix of item–item similarities, and then assigns a location to each item in *N*-dimensional space, where *N* is specified a priori (Bronstein et al., 2006). In this approach, initially neither the number nor the members of each subgroup were known. The aim of this analysis was to identify areas containing similar phytoplankton communities by comparing the abundance and biovolume data for each station and 2 depths levels: at surface and SCM (subsurface chlorophyll maximum) levels.

With evidence of temporal, vertical, and horizontal differences in the abundance of microalgal taxa as well as depth integrated biovolume ($\mu m^3\,L^{-1}$) at surface and SCM layers across the area of investigation, multidimensional scaling analysis identified distinct phytoplankton assemblages. A two-dimensional MDS configuration with superimposed clusters at Bray–Curtis similarity levels using 40% of the available biovolume data as factors is used since this threshold provides more striking results. Each plot provided respective stations for each cluster at both the surface and SCM depth from 37 stations.

From analysis of the MDS plots resulting from the additive trees clustering method, five clusters were identified (Fig. 9): Cluster 1 (Bering Sea—including its deep sea and shelf region), Cluster 2 (Bering Strait and the southern Chukchi Sea), Cluster 3 (central and northern Chukchi Sea), and Cluster 4 (Canadian Basin).

Cluster 1 included 11 stations (BR03–NB21) in the Bering Sea. This cluster is characterized by high temperature, pico-sized phytoplankton dominating, and the appearance of many dinoflagellates with, on average, $4.21 \times 10^8\ \mu m^3\,L^{-1}$ biovolume at the surface. There was no ice cover and the biovolume was higher at SCM depth than at the surface.

Cluster 2 included stations BS01–R03 (4 stations) that were located in the Bering Strait. As for biovolume, diatoms had a very high ratio (83% at surface and 89% at SCM depth). This cluster was characterized by high biodiversity and evenness with high biovolume ($1.80 \times 10^9\ \mu m^3\,L^{-1}$ biovolume at the surface). These areas experienced almost complete ice cover, whereas temperature and salinity were similar to adjacent regions.

Cluster 3 included 6 stations (R05–R15) that represent the south of the Chukchi Sea. This cluster comprised the subsurface population of pico-sized phytoplankton (surface), and nano-sized phytoplankton (SCM) accounted for the higher abundance. As for biovolume, diatoms had a higher portion (surface: 50.0% and SCM: 68.4%) similar to the Bering Strait (surface: 83.1% and SCM: 88.9%). This cluster was characterized by $4.57 \times 10^8\ \mu m^3\,L^{-1}$ of the average biovolume. Phytoplankton abundance and biovolume were lower, probably due to sea ice cover.

Cluster 4 was found at stations (M06–B85) in the northern Chukchi Sea and Canadian Basin. This cluster included the subsurface population of pico-sized phytoplankton at both depths. This cluster was characterized by low abundances and biovolume with $2.07 \times 10^8\ \mu m^3\,L^{-1}$ biovolume at the surface. The associated area was characterized by sea ice cover at all stations and lower average temperatures and salinities than at the stations of the other clusters.

Cluster 5 included 3 stations (BR23–BR02) belonging to the southern Bering Sea. This cluster shows the characteristics of northern Pacific waters with typically elevated temperatures.

Phytoplankton communities were shaped by environmental factors such as temperature and nutrients. We were able to identify 5 clusters characterized by different hydrodynamic regimes. However, our transect samples covered only a period of about 6 weeks. For this reason we had only a comparatively short time window during the summer period in 2008, and thus it is difficult to conclude any expected seasonal successional change. According to Wang et al. (2005), there are successional seasonal changes that contribute substantially to the intraanual variability of community structure and biomass (Michel et al., 2006). As sea ice melts during spring and summer, phytoplankton development tends to bloom further north (Mei et al., 2002) towards the Chukchi Sea where phytoplankton biomass builds up even until September.

4. Conclusions

High-latitude marine ecosystems are particularly sensitive to climate change because small temperature differences can have large effects on the extent and thickness of sea ice (Holland et al., 2006). The Arctic Ocean shows a reduction of the sea ice thickness and a decrease in its extent, demonstrated in the Canadian Arctic (Comiso et al., 2008). Rising air temperature and the resulting reduced multi-year ice cover will even increase the width of the seasonal ice zone reaching farther north into the Arctic Ocean in late summer (Serreze et al., 2007). The upper water column stratification will be strengthened by solar heating and increased freshwater inputs from melting sea ice and glaciers, excess net precipitation, and increased river discharge (Peterson et al., 2002). The increased stratification can also decrease the nutrient supply from deeper waters. However, with reduced sea ice cover, increased winds may also deepen the mixed layer at the surface (Carmack and Wassmann, 2006), enhancing the nutrient supply, but also decreasing light available for phytoplankton (Smetacek and Nicol, 2005; Behrenfeld et al., 2006; Wassmann et al., 2006). Recently, Li et al. (2009) found small phytoplankton thriving in the Arctic Ocean although there has been no change in total phytoplankton biomass. However, based on cell abundance and biovolume, we found a large difference in the contribution of small phytoplankton cells to the total communities in the different regions of the Arctic Ocean. Although pico- and nano-sized phytoplankton were important contributors to increased cell abundance in the study area, their chlorophyll *a* contents and biovolumes were not higher than those of larger micro-sized cells. Our results indicate that micro-sized phytoplankton such as smaller diatoms and Prymneosiophyceae contributed most to the biovolume in largely ice-free waters in the western Arctic Ocean during summer 2008. A long-term monitoring study for detecting changes in phytoplankton community and different potential contributions of various phytoplankton species will be

necessary for assessing current and ongoing environmental changes in the Arctic Ocean.

Acknowledgments

This research was supported by grants from KOPRI (PM10040) and partially the Korea Research Foundation (KRF) grant funded by the Korea government (MEST) (No. 2011-0007761). We thank the captain, crews and colleagues on board the R.V. *Xuelong*. We are also grateful to Dr. Jianfeng He for providing us with the CTD data. We are especially indebted to Dr. J.S. Park in the Korea Ocean Research and Development Institute, Mrs. M.S. Yun at the Korea Polar Research Institute and Mr. J.S. Park at Sangmyung University for assistance in the analysis of data. We very much appreciate the constructive comments by anonymous reviewers that greatly improved an earlier version of the manuscript.

References

Agawin, N.S.R., Duarte, C.M., Agusti, S., 2000. Nutrient and temperature control of the contribution of picoplankton to phytoplankton biomass and production. Limnology and Oceanography 45, 591–600.

Aizawa, C., Tanimoto, M., Jordan, R.W., 2005. Living diatom assemblages from North Pacific and Bering Sea surface waters during summer 1999. Deep-Sea Research II 52, 2186–2205.

Ardyna, M., Gosselin, M., Michel, C., Poulin, M., 2008, Spatio-temporal variability of phytoplankton production and biomass in the High Canadian Arctic in summers 2005 to 2008. Arctic Change 2008 Symposium.

Behrenfeld, M.J., O'Malley, R.T., Siegel, D.A., McClain, C.R., Sarmiento, J.L., Feldman, G.C., Milligan, A.J., Falkowski, P.G., Letelier, R.M., Boss, E.S., 2006. Climate-driven trends in contemporary ocean productivity. Nature 444, 752–755.

Bell, T., Kalff, J., 2001. The contribution of picophytoplankton in marine and freshwater systems of different trophic status and depth. Limnology and Oceanography 46, 1243–1248.

Bérard-Therriault, L., Poulin, M., Bossé, L., 1999. Guide d'identification du phytoplancton marin de l'estuaire et du golfe du Saint-Laurent incluant également certains protozoaires. Conseil national de researches du Canada, Ottawa.

Booth, B.C., 1993. Estimating cell concentration and biomass of autotrophic plankton using microscopy. In: Kemp, P.F., Sherr, B.F., Sherr, E.B., Cole, J.J. (Eds.), Handbook of Methods in Aquatic Microbial Ecology. Lewis Publishers, Boca Raton, pp. 199–205.

Booth, B.C., Larouche, P., Bélanger, S., Klein, B., Amiel, D., Mei, Z.P., 2002. Dynamics of *Chaetoceros socialis* blooms in the North Water. Deep-Sea Research II 49, 5003–5025.

Bronstein, A.M., Bronstein, M.M., Kimmel, R., 2006. Generalized multidimensional scaling: a framework for isometry-invariant partial surface matching. Proceedings of the National Academy of Sciences 103 (5), 1168–1172.

Carmack, E., Wassmann, P., 2006. Food webs and physicalbiological coupling on pan-Arctic shelves: unifying concepts and comprehensive perspectives. Progress in Oceanography 71, 446–477.

Chen, M., Huang, Y., Cai, P., Guo, L., 2003. Particulate organic carbon export fluxes in the Canada Basin and Bering Sea as derived from $^{234}Th/^{238}U$ disequilibria. Arctic 56, 32–44.

Clarke, K.R., Warwick, R.M., 1994. Change in Marine Communities: An Approach to Statistical Analysis and Interpretation. Plymouth Marine Laboratory, Plymouth.

Coachman, L.K., Aagaard, K., Tripp, R.B., 1975. Bering Strait: The Regional Oceanography. University of Washington Press, Seattle, Washington.

Codipoti, L.A., Flagg, C., Kelly, V., Swift, J.H., 2005. Hydrographic conditions during the 2002 SBI process experiments. Deep-Sea Research II 52, 3199–3226.

Comiso, J.C., 2002. A rapidly declining Arctic perennial ice cover. Geophysical Research Letters 29, 1956.

Comiso, J.C., Parkinson, C.L., Gersten, R., Stock, L., 2008. Accelerated decline in the Arctic sea ice cover. Geophysical Research Letters 35, L01703. doi:10.1029/2007GL031972.

Crumpton, W.G., 1987. A simple and reliable method for making permanent mounts of phytoplankton for light and fluorescence microscopy. Limnology and Oceanography 32, 1154–1159.

Grebmeier, J.M., Cooper, L.W., Feder, H.M., Sirenko, B.I., 2006a. Ecosystem dynamics of the Pacific-influenced northern Bering and Chukchi Seas in the Amerasian Arctic. Progress in Oceanography 71, 331–361.

Grebmeier, J.M., Overland, J.E., Moore, S.E., Farley, E.V., Carmack, E.C., Cooper, L.W., Frey, K.E., Helle, J.Z., McLaughlin, F.A., McNutt, S.L., 2006b. A major ecosystem shift in the northern Bering Sea. Science 311, 1461–1464.

Hill, V., Cota, G., 2005. Spatial patterns of primary production on the shelf, slope and basin of the Western Arctic in 2002. Deep-Sea Research II 52, 3354–3369.

Hill, V., Cota, G., Stockwell, D., 2005. Spring and summer phytoplankton communities in the Chukchi and Eastern Beaufort Seas. Deep-Sea Research II 52, 3369–3385.

Holland, M.M., Bitz, C.M., Hunke, E.C., Lipscomb, W.H., Schramm, J.L., 2006. Influence of the sea ice thickness distribution on polar climate in CCSM3. Journal of Climate 19, 2398–2414.

Ingram, R.G., Bâcle, J., Barber, D.G., Gratton, Y., Melling, H., 2002. An overview of physical processes in the North Water. Deep-Sea Research II 49, 4893–4906.

Jung, S.W., Joo, H.M., Park, J.S., Lee, J.H., 2009. Development of a rapid and effective method for preparing delicate dinoflagellates for scanning electron microscopy. Journal of Applied Phycology 22, 313–317.

Kang, S.H., Fryxell, G.A., 1991. Most abundant diatom species in water column assemblages from five ODP Leg 119 drill sites in Prydz Bay, Antarctica: distributional patterns. In: Barron, J., Larsen, B. (Eds.), Proceedings of the ODP Scientific Results, vol. 119. Ocean Drilling Program, College Station, TX, pp. 645–666.

Kang, S.H., Fryxell, G.A., Roelke, D.L., 1993a. *Fragilariopsis cylindrus* compared with other species of the diatom family Bacillariaceae in Antarctic marginal ice-edge zones. Nova Hedwigia, Beiheft 106, 335–352.

Kang, S.H., Suk, M.S., Chung, C.S., Nam, S.Y., Kang, C.Y., 1993b. Phytoplankton populations in the western Bransfield Strait and the southern Drake Passage, Antarctica. Korean Journal of Polar Research 4, 29–43.

Lassen, M.K., Nielsen, K.D., Richardson, K., Garde, K., Schlüter, L., 2010. The effects of temperature increases on a temperate phytoplankton community—a mesocosm climate change scenario. Journal of Experimental Marine Biology and Ecology 383, 79–88.

Lee, S.H., Whitledge, T.E., Kang, S.H., 2007. Recent carbon and nitrogen uptake rates of phytoplankton in Bering Strait and the Chukchi Sea. Continental Shelf Research 27, 2231–2249.

Li, W.K.W., McLanughlin, F.A., Lovejoy, C., Carmack, E.C., 2009. Smallest algae thrive as the Arctic Ocean freshens. 2009. Science 326, 539.

Macklin, S.A., Radchenko, V.I., Saitoh, S., Stabeno, P.J., 2002. Variability in the Bering Sea ecosystem. Progress in Oceanography 22, 1–4.

Martin, J., Tremblay, J-E., Gagnon, J., Tremblay, G., Lapoussiere, A., Jose, C., Poulin, M., Gratton, Y., Michel, C., 2010. Prevalence, structure and properties of subsurface chlorophyll maxima in Canadian Arctic waters. Marine Ecology Progress Series 412, 69–84.

Mei, Z.P., Legendre, L., Gratton, Y., Tremblay, J.É., LeBlanca, B.C., Mundy, C.J., Klein, B., Gosselin, M., Larouche, P., Papakyriakou, T.N., Lovejoy, C., von Quillfeldt, C.H., 2002. Physical control of spring–summer phytoplankton dynamics in the North Water, April–July 1998. Deep-Sea Research II 49, 4959–4982.

Menden-Deuer, S., Lessard, E.J., 2000. Carbon to volume relationships for dinoflagellates, diatoms, and other protist plankton. Limnology and Oceanography 45 (3), 569–579.

Michel, C., Ingram, R.G., Harris, L.R., 2006. Variability in oceanographic and ecological processes in the Canadian Arctic Archipelago. Progress in Oceanography 71, 379–401.

Nona, S.R., Agawin, N.S.R., Duarte, C.M., Agusti, S., 2000. Nutrient and temperature control of the contribution of picoplankton to phytoplankton biomass and production. Limnology and Oceanography 45, 591–600.

Olson, M.B., Strom, S.L., 2002. Phytoplankton growth, microzooplankton herbivory and community structure in the southeast Bering Sea: insight into the formation and temporal persistence of an *Emiliania huxleyi* bloom. Deep-Sea Research II 49, 5969–5990.

Parsons, T.R., Maita, Y., Lalli, C.M., 1984. A Manual of Chemical and Biological Methods for Seawater Analysis. Pergamon Press, New York 173 pp.

Peterson, B.J., Holmes, R.M., McClelland, J.W., Vörösmarty, C.J., Lammers, R.B., Ratkova, T.N., Wassmann, P., 2002. Seasonal variation and spatial distribution of phyto- and protozooplankton in the central Barents Sea. Journal of Marine Systems 38, 47–75.

Roach, A.T., Aagaard, K., Pease, C.H., Salo, S.A., Weingartner, T., Pavlov, V., Kulakov, M., 1995. Direct measurements of transport and water properties through Bering Strait. Journal of Geophysical Research 100, 18443–18457.

Serreze, M.C., Holland, M.M., Stroeve, J., 2007. Perspectives on the Arctic's shrinking sea-ice cover. Science 315, 1533–1536.

Sherr, E.B., Sherr, B.F., Wheeler, P.A., Thompson, K., 2003. Temporal and spatial variation in stocks of autotrophic and heterotrophic microbes in the upper water column of the central Arctic Ocean. Deep-Sea Research I 50, 557–571.

Shiklomanov, A.I., Shiklomanov, I.A., Rahmstorf, S., 2002. Increasing river discharge to the Arctic Ocean. Science 298, 2171–2173.

Shiomoto, A., Saitoh, S.I., Imai, K., Toratani, M., Ishida, Y., Sasaoka, K., 2002. Interannual variation in phytoplankton biomass in the Bering Sea basin in the 1990s. Progress in Oceanography 55, 147–163.

Shirshov, P.P., 1982. Plankton of the Arctic Waters. Nauka Publishing, Moscow in Russian.

Sieburth, J.M., Smetacek, V., Lenz, J., 1978. Pelagic ecosystem structure: heterotrophic compartments of the plankton and their relationship to plankton size fractions. Limnology and Oceanography 23, 1256–1263.

Smetacek, V., Nicol, S., 2005. Polar ocean ecosystems in a changing world. Nature 437, 362–368.

Sokal, R.R., Rohlf, F.J., 1995. Biometry: The Principles and Practice of Statistics in Biological Research, 3rd ed. W.H. Freeman, New York.

Springer, A.M., McRoy, C.P., 1993. The paradox of pelagic food webs in the northern Bering-Sea. III. Patterns of primary production. Continental Shelf Research 13, 575–599.

Springer, A.M., McRoy, C.P., Flint, M.V., 1996. The Bering Sea Green Belt: shelf-edge processes and ecosystem production. Fisheries Oceanography 5, 205–223.

Strathmann, R.R., 1967. Estimating the organic carbon content of phytoplankton from cell volume, cell area or plasma volume. Limnology and Oceanography 12, 411–418.

Sukhanova, I.N., Flint, M.V., Pautova, L.A., Stockwell, D.A., Grebmeier, J.M., Sergeeva, V.M., 2009. Phytoplankton of the western Arctic in the spring and summer of 2002: structure and seasonal changes. Deep-Sea Research II 56, 1223–1236.

Sukhanova, I.N., Flint, M.V., Whitledge, T.E., Stockwell, D.A., Rho, T.K., 2006. Mass development of the planktonic diatom *Proboscia alata* over the Bering Sea shelf in the summer season. Oceanology 46, 220–237.

Sun, J., Liu, D., 2003. Geometric models for calculating cell biovolume and surface area for phytoplankton. Journal of Plankton Research 25, 1331–1346.

Thomson, R.E., Fine, I.V., 2003. Estimating mixed layer depth from oceanic profile data. Journal of Atmospheric and Oceanic Technology 20, 319–329.

Tomas, C.R., 1997. Identifying Marine Phytoplankton. Academic Press, San Diego, CA.

Tremblay, J.É., Gagnon, J., 2009. The effects of irradiance and nutrient supply on the productivity of Arctic waters: a perspective on climate change. In: Nihoul, J.C.J., Kostianoy, A.G. (Eds.), Influence of Climate Change on the Changing Arctic and Subarctic Conditions. NATO Science for Peace and Security Series-C: Environmental Security, pp. 73–93.

Wang, D., Henrichs, S.M., Guo, L., 2006. Distributions of nutrients, dissolved organic carbon and carbohydrates in the western Arctic Ocean. Continental Shelf Research 26, 1654–1667.

Wang, J., Cota, G.F., Comiso, J.C., 2005. Phytoplankton in the Beaufort and Chukchi Seas: distribution, dynamics, and environmental forcing. Deep-Sea Research II 52, 3355–3368.

Wassmann, P., Reigstad, M., Haug, T., Rudels, B., Carroll, M.L., Hop, H., Gabrielsen, G.W., Falk-Petersen, S., Denisenko, S.G., Arashkevich, E., Slagstad, D., Pavlova, O., 2006. Food webs and carbon flux in the Barents Sea. Progress in Oceanography 71, 232–287.

Weingartner, T.J., Aagaard, K., Woodgate, R.A., Danielson, S., Sasaki, Y., Cavalieri, D., 2005. Circulation on the north central Chukchi Sea shelf. Deep-Sea Research II 52, 3150–3174.

Zapata, M., Rodríguez, F., Garrido, J.L., 2000. Separation of chlorophylls and carotenoids from marine phytoplankton: a new HPLC method using a reversed phase C8 column and pyridine-containing mobile phases. Marine Ecology Progress Series 195, 29–45.